scientific reports

Check for updates

OPEN

Higher sodium in older individuals or after stroke/reperfusion, but not in migraine or Alzheimer's disease – a study in different preclinical models

Chenchen Xia[1], Wangde Dai[2], Juan Carreno[2], Andrea Rogando[1], Xiaomeng Wu[3], Darren Simmons[3], Natalie Astraea[3], Nathan F. Dalleska[4], Alfred N. Fonteh[5], Anju Vasudevan[6], Xianghong Arakaki[1]✉ & Robert A. Kloner[2]

Sodium serves as one of the primary cations in the central nervous system, playing a crucial role in maintaining normal brain function. In this study, we investigated alterations in sodium concentrations in the brain and/or cerebrospinal fluid across multiple models, including an aging model, a stroke model, a nitroglycerin (NTG)-induced rat migraine model, a familial hemiplegic migraine type 2 (FHM2) mouse model, and a transgenic mouse model of Alzheimer's disease (AD). Our results reveal that older rats exhibited higher sodium concentrations in cerebrospinal fluid (CSF), plasma, and various brain regions compared to their younger counterparts. Additionally, findings from the stroke model demonstrated a significant increase in sodium in the ischemic/reperfused region, accompanied by a decrease in potassium and an elevated sodium/potassium ratio. However, we did not detect significant changes in sodium in the NTG-induced rat migraine model or the FHM2 mouse model. Furthermore, AD transgenic mice showed no significant differences in sodium levels compared to wild-type mice in CSF, plasma, or the hippocampus. These results underscore the nuanced regulation of sodium homeostasis in various neurological conditions and aging, providing valuable insights into potential mechanisms underlying these alterations.

Keywords Sodium, CSF, Aging, Stroke, Neurological disease, Na^+/K^+-ATPase

Ion channel dysfunction can cause numerous nerve or muscle disorders, including epilepsy, hemiplegic migraine, hyperekplexia and myotonia[1]. Some of these diseases share a common characteristic: they usually manifest as normal neurological function with paroxysmal disease attacks[2]. This is due to the central neural circuit's ability to maintain the stability and plasticity of the brain; both chemical signals and ion transportation play a vital role in this regulation[2,3]. Cerebrospinal fluid sodium (CSF) could also affect the ion concentration in brain parenchyma, as the CSF can exchange fluid and ions with interstitial fluid (ISF) by the perivascular spaces[4]. This suggests that the homeostasis of ions in the brain and CSF are both crucial for maintaining normal brain function.

Sodium is the main cation of extracellular fluid, while potassium is the primary intracellular cation[5,6]. In addition to their role in maintaining fluid levels and osmolality, sodium and potassium gradients are essential for the resting potential and the generation of action potentials[7,8]. Membrane voltage changes can activate voltage-gated sodium channels (VGSCs), directly associated with the ionic gradient between intra- and extracellular environments[9,10]. Although the shape or speed of action potentials may vary in different types of cells, it is evident that VGSCs initiate the inward current during the rising phase of the action potential[11]. This means that

[1]Cognition and Brain Integration Laboratory, Neurosciences Department, Huntington Medical Research Institutes, Pasadena, CA, USA. [2]Cardiovascular Department, Huntington Medical Research Institutes, Pasadena, CA, USA. [3]Analytical Biochemistry Core, Huntington Medical Research Institutes, Pasadena, CA, USA. [4]Water and Environment Laboratory, California Institute of Technology, Pasadena, CA, USA. [5]Biomarker and Neuro-Disease Mechanism Laboratory, Neurosciences Department, Huntington Medical Research Institutes, Pasadena, CA, USA. [6]Angiogenesis and Brain Development Laboratory, Department of Neurosciences, Huntington Medical Research Institutes, Pasadena, CA, USA. ✉email: xianghong.arakaki@hmri.org

the modulation in sodium concentration can directly influence the excitability of the central nervous system. Ionic balance is crucial for maintaining the stability of brain function; changes of extracellular or intracellular ion gradient can affect the neuron excitability and even lead to brain diseases[12–14].

Sodium changes have been reported in neurological conditions including stroke, aging, dementia, and migraine. It is known that excessive salt intake is associated with a higher risk of hypertension, and hypertension will contribute to stroke, kidney diseases, and cardiovascular diseases[15–17]. Sodium magnetic resonance imaging (MRI) has revealed increased signal intensity in ischemic areas in animal stroke models, and the relative sodium signal is related to the onset time of stroke in acute patients, suggesting that sodium could serve as a new biomarker for analyzing stroke progression[18–20]. Stroke and hypertension were usually seen in the aging cohort compared to young individuals[21–23]. High sodium diet can link to higher risk of dementia, and animal work shows that the overdose of sodium can induce an immune response in the gut and promote the cognitive impairment[24]. In vitro study also proves that high sodium treatment can increase the Aβ levels in HEK293 cells as it can suppress the Aβ clearance in the cell[25]. Previous research found elevated sodium levels in the CSF during migraine attacks in migraine patients, without any changes of osmolality or other ion concentrations[26]. Furthermore, the total sodium concentration in the entire brain was also elevated in patients with Huntington's disease, especially in the bilateral striatum, which is a crucial area for Huntington's disease[27]. Beside these, various models have demonstrated that intracellular sodium increased during hypertrophy, heart failure and ischemia–reperfusion, and the elevated sodium levels during heart failure are primarily due to increased sodium influx rather than decreased sodium efflux[28,29]. All these findings emphasize the connection between sodium fluctuations and different diseases, underscoring the importance of investigating the role of sodium in different disease models. However, most studies explored global sodium changes in the brain through MRI[18–20]. Sodium levels have not been directly determined in the CSF or brain of various preclinical neurological models.

In this study, we induced different neurological disease models, including aging, stroke, Alzheimer's disease, and two different migraine models to determine if sodium and potassium concentration fluctuated by genders in the CSF, plasma, and different brain regions in these models of neurological diseases. Our results show cation changes in a stroke and aging model but not in migraine and Alzheimer's disease models, thus underscoring nuanced sodium homeostasis and providing valuable insights into potential mechanisms underlying these neurological models.

Materials and methods

This study is performed in accordance with relevant guidelines and regulations. This study is reported in accordance with ARRIVE guidelines.

Animals

For the aging model, 2–3 months and 18-month-old SD Sprague Dawley (SD) rats were purchased from Envigo (Inotiv Inc., West Lafayette, IN). For the stroke and acute migraine model, 2–3 months SD rats were also purchased from Envigo. For the chronic migraine study, Familial hemiplegic migraine type 2 (FHM2) heterozygous mice ($Atp1a2^{+/R887}$) were kindly provided by Dr. Brennan (University of Utah) and bred at Huntington Medical Research Institutes (HMRI)[30]. For the Alzheimer's disease (AD) model, 6–7 months double transgenic AD mice (B6.Cg-Tg(APPswe,PSEN1dE9)85Dbo/Mmjax) were purchased from the Jackson Laboratory (Bar Harbor, ME). Animals were housed in a temperature and humidity-controlled room under a 12 h light–dark cycle. Water and food were provided ad libitum. All animals were habituated for at least 1 week before use for experimental procedures. A total of 85 SD rats, and 68 mice were used for this study. Animal experiments were in full compliance with the NIH Guide for Care and Use of Laboratory Animals and were approved by the HMRI Institutional Animal Care Committees.

Aging rat model and sample collection

12 (6 males and 6 females) 2–3 month-old SD rats were used for the young animal group, and 22 (12 males and 10 females) 18 month-old SD rats were used for the old animal group. Lab rats can live around 2.5–3 years total, therefore 2–3 months rat are considered the equivalent of young adult humans, while 18-month-old rats represent approximately 45–50 human years[31–33]. Animals were deeply anesthetized with ketamine (90 mg/kg) and xylazine (10 mg/kg) by an intraperitoneal (IP) injection and placed on a stereotaxic instrument on the heating pad. After the neck skin was shaved, the CSF collection site was swabbed with 10% povidone-iodine, followed by 70% ethanol. A sagittal incision was made in the skin below the occiput. Subsequently, subcutaneous tissue and muscles were separated through blunt dissection using forceps, with the muscles held apart. A glass capillary needle was introduced through the dura mater into the cisterna magna to collect CSF samples. Each animal yielded a CSF sample ranging from 100 to 150 µL. For whole blood collection, 1 mL was obtained through cardiac puncture under deep anesthesia and placed in EDTA-treated tubes. The collected blood was then subjected to a 15 min centrifugation at 2000 g and 4 °C to obtain the plasma supernatant. Rats were euthanized via decapitation (while under deep anesthesia), and the choroid plexus, cerebellum, hippocampus, and the rest of the brain were collected separately. All samples were stored in a − 80 °C freezer until further tests.

Stroke rat model and sample collection

A total of 8 female and 12 male 2–3 months SD rats were used for the stroke study. The rat model of transient middle cerebral artery occlusion was established according to the method described by Uluç et al.[34]. In brief, the rats were anesthetized by an intraperitoneal injection of ketamine (90 mg/kg) and xylazine (10 mg/kg). The hair over the neck area was removed and the skin was cleaned with 70% alcohol. The rat was placed on a water circulating heating pad to prevent hypothermia and the rectal temperature was monitored and maintained around

37 °C. The rat was intubated and mechanically ventilated with room air with a tidal volume of 1 ml/100 g body weight at 60 cycles per minute. A surgical incision was performed to expose the right carotid artery. The common carotid artery was temporarily occluded while a suture (4-0 Silicone rubber-coated monofilament purchased from Doccol Corporation, Redlands, CA) was introduced into the internal carotid artery and advanced 20 mm until it interrupted the blood supply to the middle cerebral artery. The suture was left in place for 60 min and then at the end of the 60 min it was removed. Reperfusion was allowed for 3 h.

Rats were euthanized via decapitation (under deep anesthesia) and the brain was collected for analysis to assess the anatomic size of the cerebral infarction. The brain was carefully removed from the skull. The brain was placed into the rat brain slice matrix to slice the brain into even segments. The brain was sliced into 2 mm coronal segments using razor blades. There were 6 segments when finished. Segments 1, 3, and 5 of the brain were placed into 1% 2,3,5-triphenyltetrazalium chloride (TTC) solution in a water bath at 37 °C for 15 min to visualize the stroke (pale white area). We ensured that the TTC solution completely covered the tissue segments. TTC stains viable brain tissue brick red and the infarct appears as a pale white area (Fig. 2A–B). For brain tissue ion measurements, segments 2, 4 and 6 the opposing block faces from the slices that were stained with TTC) were kept on ice for collection of the brain viable and necrotic tissue based on the TTC staining pictures of segments 1, 3, and 5. The same region from the contralateral side was also collected as their own control group. The sham group has the same surgery, TTC staining and collection procedures as the stroke group but without the occlusion step. All the samples were kept in a − 80 °C freezer for further tests.

Migraine rat model and sample collection

A total of 14 female and 17 male 2–3 months SD rats were used for the migraine study. Animals were anesthetized by isoflurane (5%) and then fastened to a stereotaxis apparatus with continuous isoflurane vapor (1.5–2%). A heating pad was placed under the animal to maintain the body temperature around 37 °C. The body temperature and ECG of the animals were monitored throughout the surgery. Around 20 µL CSF were collected from the cisterna magna before treatment as baseline (as described in the aging rat model part). 10 mg/kg nitroglycerin (NTG) or the same volume of saline (control) was used to induce migraine or control by IP injection. From the cisterna magna, around 20 µL CSF and 100 µL CSF were collected at 30 min and 2 h post-administration, respectively. The animals were euthanized via decapitation (under deep anesthesia) at 2 h post-administration and plasma, choroid plexus, cerebellum, and the rest of the brain were collected. All samples were stored in a freezer at -80 °C until chemical analyses were performed.

Familial hemiplegic migraine type 2 (FHM2) transgenic mice model and sample collection

A total of 16 female and 16 male 3–6 months heterozygous mice ($Atp1a2^{+/R887}$) and their wild-type (WT) littermates were used for the study. Animals were anesthetized with ketamine (90 mg/kg) and xylazine (10 mg/kg) cocktail via IP injection. 2–5 µL CSF and about 0.5 mL whole blood (to get plasma as previously described) were collected from each mouse. Mice were euthanized via decapitation (under deep anesthesia) and cerebellum, and the rest of the brain were collected and kept at − 80 °C as previously described.

Alzheimer's disease (AD) transgenic mice model and sample collection

16 female and 20 male 6–7 months Alzheimer's disease (AD) APP/PS1 double transgenic mice (B6.Cg-Tg(APPswe,PSEN1dE9)85Dbo/Mmjax) and their wild-type (WT) littermates were used for AD study. Animals were anesthetized via IP injection with ketamine (90 mg/kg) and xylazine (10 mg/kg) cocktail. 2–10 µL CSF and about 0.5 mL whole blood (to get plasma as previously described) were collected from each mouse. Mice were euthanized via decapitation (under deep anesthesia), and hippocampus and the rest of the brain were collected and kept at − 80 °C as previously described.

Ion chromatography for sodium measurement

CSF and plasma samples stored in a − 80 °C freezer were thawed on ice. Deionized ultra-pure water was added to brain samples at a concentration of 0.05 g/mL. The tissue was then homogenized using an ultrasonic cell disruptor (Branson 450 Sonifier, VWR, Radnor, PA) at a speed of 2 (output with Constant Duty Cycle) for 5 s (× 5 or until total disruption of the tissues). The resulting homogenate was centrifuged at 13,000 rcf for 10 min, and the supernatant was filtered (0.2 µm PTFE) and frozen at − 80 °C for subsequent ion chromatography (IC) tests. In the present study, CSF samples were not collected from the stroke model due to the potential impact of ischemia/reperfusion injury on cerebral swelling. For all the brain samples from the stroke model, CSF samples from AD and FHM2 mice model, and brain samples from NTG-induced migraine rat model, measurements were conducted on a Dionex ICS-6000 HPIC System (Thermo Scientific, Waltham, MA). CSF was diluted 1000 times for the test, while brain samples were diluted 100 times. For the CSF, plasma and brain samples from the aging model, plasma and brain samples from AD and FHM2 mice model, and CSF and plasma from NTG-induced migraine rat model, measurements were carried out on a Dionex ICS-3000 HPIC System (Thermo Scientific, Waltham, MA). Plasma and CSF were diluted 200 times for the test, while brain samples were diluted 20 times.

A Thermo Integrion integrated ion chromatography system was used to measure cation concentrations. Thermo AS-DV autosampler configured to use 5 mL PolyVials was used to inject the diluted samples into Integrion. Cations were resolved using a CS-16A separator column (2 mm × 250 mm) protected by a CG-16A guard column (2mmx50mm, Thermofisher Scientific) maintained at 30 °C. Ultra-pure water was pumped at 0.16 mL per minute and a methanesulfonic acid solution at a constant (isocratic) concentration of 30 mM was produced using an EGC 500 MSA eluent generator cartridge (Thermofisher Scientific). Suppressed conductivity detection was achieved using a Dionex CDRS-500 2 mm suppressor operated in eluent recycle mode at 4.2 V. The conductivity detector was maintained at 35 °C. Diluted samples were loaded into Polyvials (Thermofisher

Scientific) using the caps with integral filters. The large volume of diluted sample ensured complete flushing of the system through to the approximately 5 µl sampler loop with < 1% carryover across the relevant concentration range. Data was processed using ThermoFisher Scientific Chromeleon software, version 7.2. Standard curves were generated for each species. For sodium concentration, standard measurements were fitted to a line. The standards used for brain homogenates ranged from ~ 0.01 to 0.29 mM, while the standards for CSF and plasmid ranged from ~ 0.017 to 1.16 mM to ensure the standard ranges adequately covered all sample concentrations.

Statistical analysis

All the data are presented as mean ± SD. A two-way analysis of variance (ANOVA) analysis was used to assess differences in CSF samples between saline and NTG-treated rats in the acute migraine model. Unpaired t-tests and Mann–Whitney tests were used as appropriate for all the other samples in different models to compare the sodium (and potassium) changes between the control and disease group. False discovery rate was used for multiple testing correction and $p < 0.05$ was considered statistically significant. All the statistical analyses and figures were performed using GraphPad Prism 9 (GraphPad Software, Boston, MA).

Results

Sodium levels were higher in the CSF, plasma and some brain regions in older rats compared to younger rats

CSF, plasma, and various brain regions were collected from 18 months and 2–3-month-old rats to investigate sodium changes in older animals compared to younger ones. In 18-months-old female rats, the sodium concentrations in both CSF and plasma were significantly higher than in the 2–3 months females ($p < 0.001$, Fig. 1A). In males, similar trends in sodium changes were observed. In CSF and plasma, the sodium concentration in 18 months males was significantly higher than in 2–3-month male rats ($p < 0.05$, and $p < 0.01$, respectively, Fig. 1B). Different brain regions, including the cerebellum, hippocampus, and the rest of the brain (e.g., cerebral cortex, subcortical regions excluding cerebellum and hippocampus) were analyzed. In females, the sodium concentration in all these regions was elevated in the 18-month group compared to the 2–3-month group ($p < 0.01$, $p < 0.01$, and $p < 0.05$ in the cerebellum, hippocampus, and rest of the brain, respectively. Figure 1C). However, in the males, elevated sodium levels were detected only in the cerebellum of 18 months group ($p < 0.01$), with no significant differences in the hippocampus or the rest of the brain between the 18 months and 2–3 months groups (Fig. 1D).

Sodium levels were higher and potassium levels were lower in the ischemic/reperfused area of stroke compared to the nonischemic areas

In this study, we collected the ischemic/reperfused region of the brain in the stroke model, the brain tissue from the contralateral region as their own control (Fig. 2A), and the brain tissue from the same side and the same region in the sham group as the sham control (Fig. 2B). The results showed that the sodium concentration in the ischemic/reperfused region of stroke in female rats was significantly higher than the contralateral side ($p < 0.001$) and sham group ($p < 0.01$), while no difference in sodium concentration between the contralateral side and the sham group (Fig. 2C). The potassium concentration showed the opposite change to sodium in the stroke group. The potassium concentration in the ischemic/reperfused region was lower than the contralateral side ($p < 0.01$) and sham group ($p < 0.05$) in females, and no difference was found between the contralateral side and the sham group (Fig. 2D). Figure 2E shows the increased sodium/potassium ratio in the ischemic region of stroke in females when compared with the contralateral side or sham group ($p < 0.01$).

In males, the sodium or potassium concentrations in the ischemic/reperfused region of stroke model (compared with contralateral regions or sham group) demonstrated similar changes as in the females. The sodium concentration was higher in the ischemic/reperfused region than in the contralateral side ($p < 0.0001$) and sham group ($p < 0.01$, Fig. 2F). The potassium concentration in the ischemic region was significantly lower than the

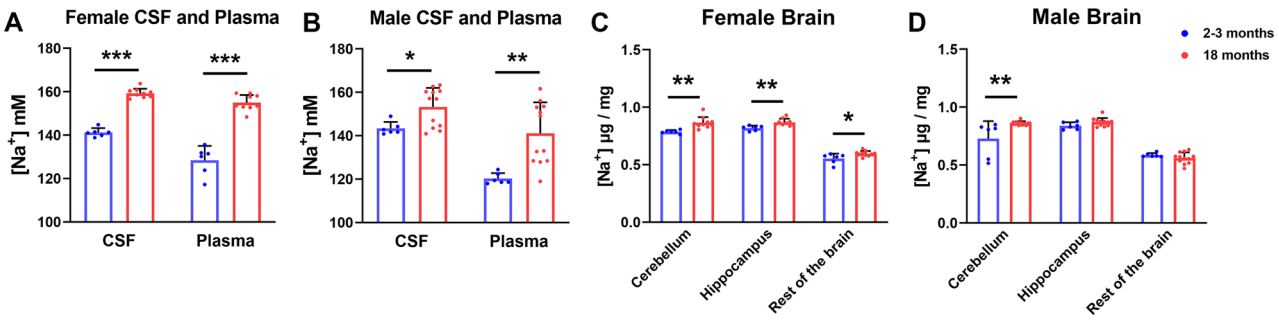

Fig. 1. Sodium measurement in 2–3 months and 18 months rats. (**A**) Sodium concentration increased in the CSF and plasma of 18-month-old females compared to 2–3-month-old females. (**B**) Sodium concentration increased in the CSF and plasma of 18-month-old males compared to 2–3-month-old males. (**C**) Sodium levels increased in the cerebellum, hippocampus, and rest of the brain in 18-month-old females. (**D**) Sodium levels increased in the cerebellum in 18 months males. n = 6 for 2–3 months females and males, n = 10 for 18 months females, n = 12 for 18 months males. Data were displayed as mean ± SD, $^{*}p < 0.05$, $^{**}p < 0.01$, $^{***}p < 0.001$.

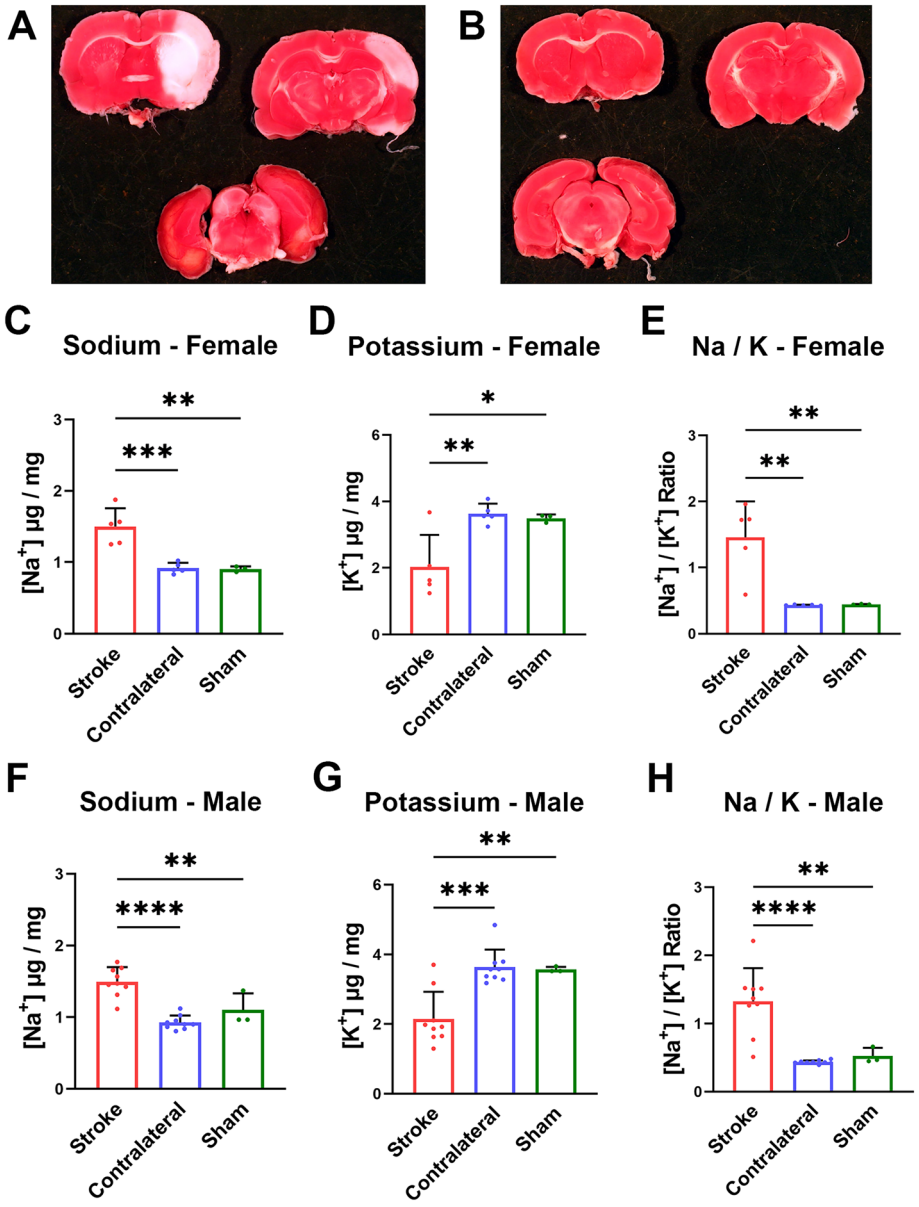

Fig. 2. Sodium and potassium measurements in stroke rats. (**A**–**B**) Example of TTC staining of male rats from stroke (**A**) and sham (**B**) group. (**C**) The sodium concentration increased in the ischemic/reperfused brain regions in female rats compared to the nonischemic regions. (**D**) In females, potassium concentration decreased in the ischemic/reperfused brain region compared to the nonischemic regions. (**E**) The sodium/potassium ratio increased in the ischemic/reperfused brain region in female rats compared to the nonsichemic regions. (**F**) The sodium concentration increased in the male rats' ischemic/reperfused brain region compared to the nonischemic regions. (**G**) In males, potassium concentration decreased in the ischemic/reperfused brain region compared to the nonischemic regions. (H) The sodium/potassium ratio increased in the ischemic/reperfused brain region in male rats compared to the nonischemic regions. n = 5 for the female stroke and contralateral group, n = 3 for the female sham group, n = 9 for the male stroke and contralateral group, and n = 3 for the male sham group. Data were displayed as mean ± SD. $^{*}p < 0.05$, $^{**}p < 0.01$, $^{***}p < 0.001$, $^{****}p < 0.0001$.

contralateral side ($p < 0.001$) and sham group ($p < 0.01$, Fig. 2G). Like the females, the male stroke group showed a higher sodium/potassium ratio in the ischemic/reperfused region when compared with the contralateral side ($p < 0.001$) and sham group ($p < 0.01$, Fig. 2H).

No sodium concentration elevations compared to baseline were detected in the CSF, plasma and brain in NTG-treated rats

The CSF samples were collected from 2 to 3-month-old rats at different time points after saline or NTG administration, including baseline, 30 min, and 2 h after NTG or saline application. In the females, no significant

differences were observed between the NTG and saline groups across time points (Fig. 3A). In plasma and different brain regions including spinal trigeminal nucleus caudalis (sp5c), ventral posterior medial and ventral posterior lateral (VPM/L), primary somatosensory cortex, cerebellum and the rest of the brain, the sodium concentration in the NTG group did not show any differences compared with the saline group (Fig. 3B–C).

In the males, the sodium concentration in the CSF from baseline, 30 min, and 2 h after NTG-treated rats were comparable with that from their saline group (Fig. 3D). However, in the plasma, the sodium concentration in the NTG group was significantly lower than the saline group ($p < 0.05$, Fig. 3E). Similar to the female rats, there was no difference in sodium levels in any of the brain regions between NTG and saline-treated rats in males (Fig. 3F). In summary, sodium changes observed were only in the plasma: sodium in the plasma of male migraine group (NTG) were decreased compared to that of the male controls (saline). No sodium changes were observed in the female plasma, or CSF or brain in either gender.

FHM2 transgenic mice had the same level of sodium in CSF, plasma and cerebellum compared to wild-type mice

In this investigation, CSF, plasma, and cerebellum were collected from 3 to 6-month-old FHM2 mice, a transgenic migraine mouse model, and their wild-type counterparts from the same litter the test. In both female and male animals, the sodium concentration in the CSF, plasma, and cerebellum of FHM2 mice exhibited similarities to that of the wild type mice (Fig. 4A–D). No significant differences were observed between female and male mice in any of the sample groups.

Alzheimer's disease (AD) transgenic mice had the same level of sodium in CSF, plasma and hippocampus compared to wild-type mice

In this study, CSF, plasma, and hippocampal samples were collected or analysis from 6 to 7-month-old Alzheimer's disease (AD) transgenic mice and their wild-type counterparts from the same litter. No significant alterations in sodium levels were observed in any of the sample groups, including both females and males, compared to control mice. This result indicates that AD transgenic mice exhibited similar sodium levels to those of wild type mice, as illustrated in Fig. 5A–D. Furthermore, no significant differences were detected between females and males within any of the sample groups.

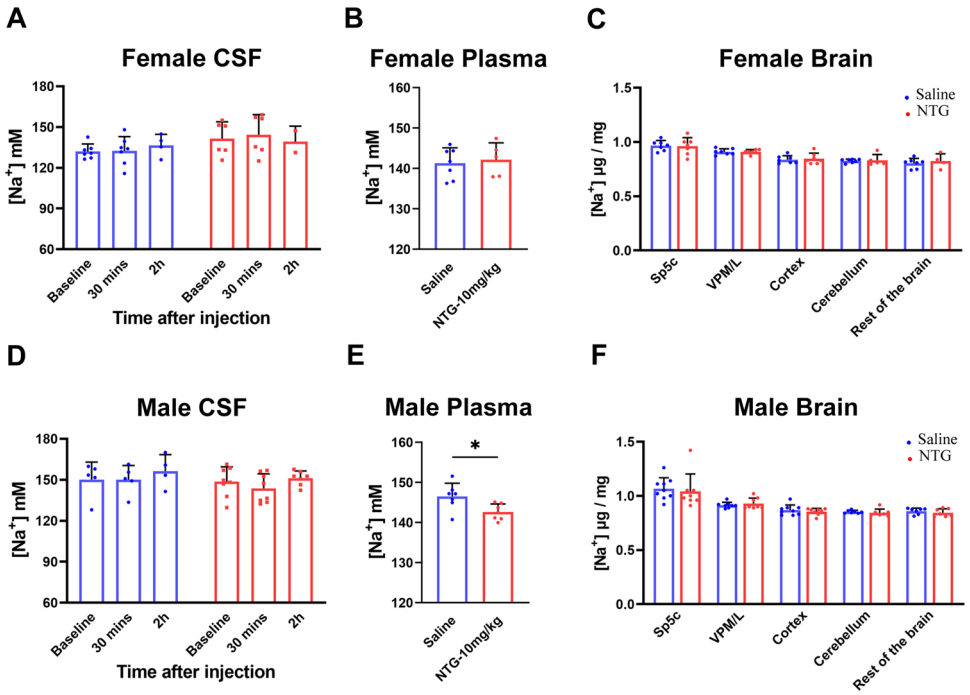

Fig. 3. Sodium measurement in NTG-treated rats. (**A**) Sodium concentration in the CSF of saline and NTG-treated female rats. (**B**) Sodium concentration in the plasma of saline and NTG-treated female rats. (**C**) Sodium concentration in the spinal trigeminal nucleus (Sp5c), ventral posteromedial nucleus and ventral posterolateral nucleus (VPM/L), somatosensory cortex, cerebellum, and rest of the brain in saline and NTG-treated female rats. (**D**) Sodium concentration in the CSF of saline and NTG-treated male rats. (**E**) Sodium concentration in the plasma of saline and NTG-treated male rats. (**F**) Sodium amount in the Sp5c, VPM/L, somatosensory cortex, cerebellum, and rest of the brain in saline and NTG-treated male rats. n = 7 for saline and NTG-treated females, n = 9 for saline treated males, n = 8 for NTG-treated males. Data were displayed as mean ± SD.

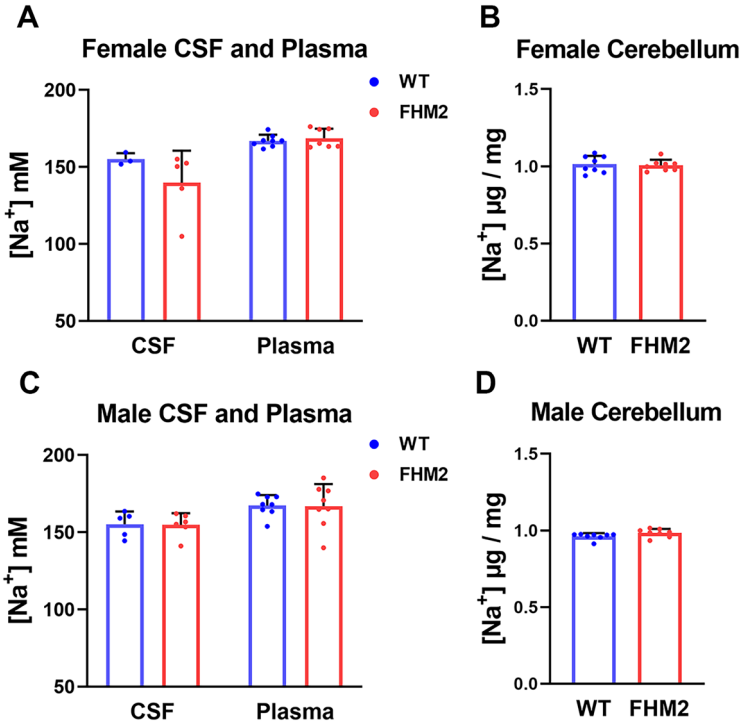

Fig. 4. Sodium measurement in FHM2 mice. (**A**) Sodium concentration in the CSF and plasma of FHM2 and WT female mice. (**B**) Sodium amount in the cerebellum of FHM2 and WT female mice. (**C**) Sodium concentration in the CSF and plasma of FHM2 and WT male mice. (**D**) Sodium amount in the cerebellum of FHM2 and WT male mice. n = 8 for each group. Data were displayed as mean ± SD.

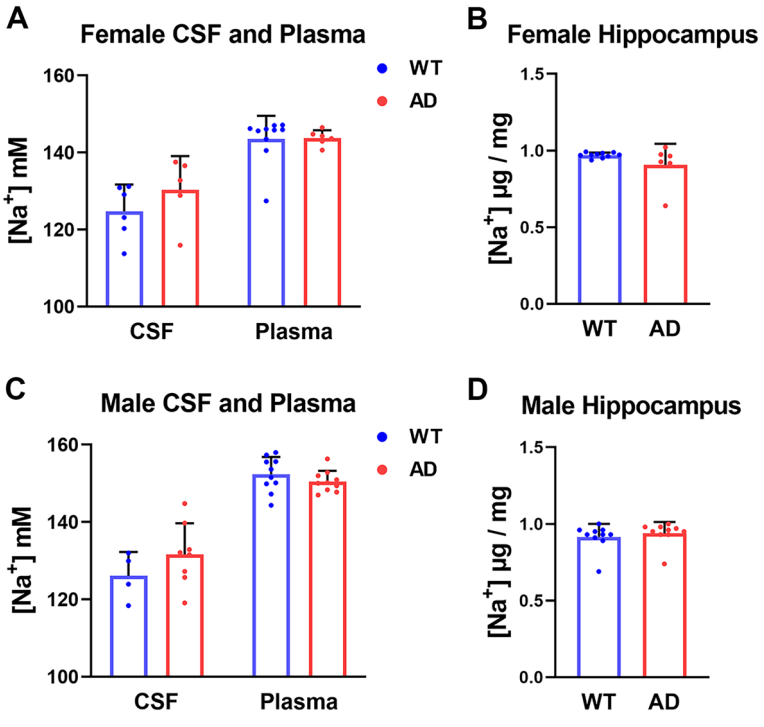

Fig. 5. Sodium measurement in AD mice. (**A**) Sodium concentration in the CSF and plasma of AD and WT female mice. (**B**) Sodium amount in the hippocampus of AD and WT female mice. (**C**) Sodium concentration in the CSF and plasma of AD and WT male mice. (**D**) Sodium amount in the hippocampus of AD and WT male mice. n = 10 for WT female and male mice, n = 6 for AD female mice, n = 10 for AD male mice. Data were displayed as mean ± SD.

Discussions

In this study, we tested whether there were changes in sodium levels in the CSF, plasma and/or regions of the brain in a wide variety of experimental neurological disease models including aging, stroke, migraine, and Alzheimer's disease. The results showed that the sodium concentration was elevated in the CSF, plasma, and some brain regions in the older rats (18 months) when compared to young rats (2–3 months), and the sodium concentration increased, while the potassium concentration was lower in the ischemic/reperfused brain area in the acute stroke model. No significant changes were detected in the CSF, plasma, or brain in our acute migraine rat model and FHM2 mice model or transgenic AD mice model.

Aging accompanied by sodium accumulation in the CSF, plasma, and brain

Aging may not belong to a disease, but it will be accompanied by an increased propensity for age-related medical and neurological diseases and the inevitable decline of cognitive functions[35]. Although studies reported age-related pathologies and biomarkers, active efforts are still needed to monitor aging and directly link them to age-related diseases[36,37]. It is well known that excessive salt intake is associated with higher plasma sodium concentration and a higher risk of hypertension, while reduced sodium intake links to lower plasma sodium and blood pressure reduction[15,38]. In hypertensive individuals, higher salt intake has been reported to increase the sodium concentration in the CSF from 145.3 ± 0.5 to 147.7 ± 0.4 mmol/L[39,40]. Similarly, in different hypertensive rat models, excessive sodium intake can raise CSF sodium levels from 152.3 to 155.2 ± 0.6 meq/L[41–43]. However, sodium concentration changes with age are not well studied to our knowledge. In this study, we focused on the central nervous system of the aging rats and found that the sodium accumulated in the CSF, plasma, and some brain regions in the older rats compared to young rats. Hypertension and stroke both increase with age[44,45]. Previous studies also showed that there is a positive relationship between age and blood pressure in rats, which contributes to the higher hypertension prevalence in the aged group[46]. Although there is no direct evidence showing that excessive sodium intake affects brain parenchyma sodium levels, high salt intake has been reported to induce endothelial dysfunction of cerebral arteries and contribute to cerebral small vessel disease (SVD), potentially impacting sodium levels in the brain parenchyma[47–49]. As we have shown, the increased sodium in the older group may increase the risk of hypertension.

It is well known that aging can lead to a decline in kidney function, the decreased ability to sodium excretion could affect sodium balance throughout the body, and contributing to hypertension and cardiovascular problems[50,51]. Additionally, the older population is more prone to dehydration due to a diminished sense of thirst, which can concentrate the sodium levels in the plasma or CSF[52–54]. Reduced fluid intake and increased fluid output (regulated by the renal system) lead to sodium dysregulation in the body in the elderly[53]. Several potential outcomes could relate to brain sodium changes. For example, sodium concentration change in the neurons could alter the voltage gated sodium channels (VGSCs) activity and neuronal excitability, while the sodium change in the astrocytes will affect the transportation of transmitters, metabolic pathways, and the homeostasis of the CNS, which may contribute to different age-related diseases[55,56]. Whether the sodium elevation is intracellular or extracellular, and the specific mechanisms of sodium elevation in aging or stroke are worth further investigation.

Sodium elevation after stroke

Previous research found that the sodium signal intensity in ischemic brain lesions of sodium magnetic resonance image (MRI) showed a linear increase after stroke onset in animal models[57,58], and the elevated sodium could be used to detect stroke and its recovery assessment[20]. It is also observed in stroke patients that the sodium intensity in the ischemic lesion progressed over time from serial data of the same patient[18]. Unlike the previous relative quantification method, we used a direct ion measurement method in this study, and the results demonstrated that the sodium concentration in the ischemic/reperfused brain region was significantly higher compared to non-ischemic brain tissue. In contrast, the potassium concentration was lower in the ischemic brain region compared to normal brain tissue. Stroke can induce cell death due to the shortage of blood supply and hypoxia can lead to ATP depletion[59]. Na^+/K^+-ATPase (NKA) is a major consumer of ATP in the brain, essential for maintaining the sodium/potassium gradient of the cell[60]. Energy deprivation can induce the failure of the NKA and increase the intracellular sodium[56,61]. Interestingly, the protein expression of NKA α1, α2, and α3 isoforms was reduced after stroke reperfusion compared with sham group[62]. In this study, the increased sodium and the reduced potassium in the ischemic brain region may be caused by the dysfunction of the NKA. Besides the ionic dysregulation (sodium changes) in the intra- and extra-cellular environment, it is also reported that stroke can reduce the influx of CSF to the brain parenchyma after 24 h in mice[63]. The change in the extracellular environment after stroke may also worsen the ionic dysregulation and cell damage in the ischemic area, making the ischemia become more dangerous and complex. In addition, intracerebroventricular (ICV) infusion of higher sodium artificial cerebrospinal fluid (aCSF) in hypertensive rats will increase the stroke onset (incidence) without changing the blood pressure, which proves that exposure to a high sodium environment will increase the risk factor for stroke[64]. Our results of sodium elevation after stroke are consistent with previous reports. All the findings hint that the normal sodium level in the brain may help to decrease the risk of stroke, and the ischemic region could not keep the ion balance due to the failure of NKA. Further study of sodium changes intra- or extra-cellular environment is worth of interests.

The sodium increase observed in the stroke/reperfusion model and aging model in this study may share some common mechanisms. For example, increased sodium in the ischemic area after stroke/reperfusion can be attributed to ischemia/reperfusion-related changes, including mitochondria dysfunction[65]. Interestingly, the sodium elevation in the aging model may also involve ischemia and mitochondria dysfunction[66]. Additionally, aging is associated with greater risk of hypertension and vascular changes, which may increase the risk of stroke.

Acute migraine, familial hemiplegic migraine and Alzheimer's disease models are not accompanied by sodium change

Previous research found that migraine patients showed higher sodium levels in the CSF, which has a positive correlation with pain levels[26,67]. However, this study did not find any sodium change in either the migraine mice model (FHM2) or the NTG-induced rat model. The model, age, or method may cause the difference. For example, we collected the CSF multiple times from the cisterna magna, which may not accurately reflect potential variations of microdomain sodium that located next to the choroid plexus. Additionally, Harrington et al. reported a modest increase in sodium levels in cerebrospinal fluid (CSF) collected by lumbar puncture. Additionally, Harrington et al. have reported that sodium level at CSF collected by lumbar puncture increased from 145 mM (controls) or 146 mM (migraine patients during interictal stage) to 149 mM (migraine patients during migraine attack), the numerical change is relatively small, underscoring the subtlety of the observed alterations[26]. The sodium change at the brain level may be more significant than at the spinal level. Similarly, Abad et al. reported sodium elevation in the NTG-treated male rodents[68]. However, no sodium changes were detected in the current study, either in males or females. The difference may be due to the temporal and spatial collection of sodium images using non-invasive MRI compared with the invasive collection of CSF from different timepoints after NTG treatment in our present IC studies. It is possible that MRI may be able to pick up subtle region or microdomain-specific sodium changes, while our method only pick up dramatic changes.

Although previous studies showed that high sodium intake correlates with worse cognition, and AD patients show higher intracellular sodium or potassium levels in the brain tissue, we did not find any sodium change in our AD mice model[69–71]. The different findings may be due to the different samples, ages, and methods used for the test. Previous tests were all performed on AD patients while we were using the AD mice model. While previous investigators introduced MRI scanning for aged patients (over 70 years old) or flame photometer for the AD brain samples (mean: 79 years old), our research group used a direct cation measurement in younger mice (6–7 months old) and did not observe a change of the sodium in the CSF, plasma, and hippocampus. Also, since age is a risk factor for AD, our cross-sectional studies may not capture temporal changes in sodium observed in our model.

To summarize the key findings, we observed an increase in sodium levels in aging rats (CSF, plasma, and brain regions) and in a stroke model (ischemic/reperfused brain region). In contrast, no sodium changes were observed in the CSF or brain in our acute migraine model induced by nitroglycerin or in a transgenic mice migraine model. Additionally, sodium was also not increased in a transgenic AD model. Therefore, despite limitations, we reported that increased sodium levels may be an outcome or have significant pathological effects on some but not all neurological conditions. Our unique method can help detect sodium changes in only specific pathological conditions.

Data availability

Data is provided within the manuscript. Correspondence and requests for materials should be addressed to X.A.

Received: 31 May 2024; Accepted: 5 September 2024
Published online: 16 September 2024

References

1. Cooper, E. C. & Jan, L. Y. Ion channel genes and human neurological disease: Recent progress, prospects, and challenges. *Proc. Natl. Acad. Sci. U. S. A.* **96**, 4759–4766 (1999).
2. Kullmann, D. M. & Waxman, S. G. Neurological channelopathies: New insights into disease mechanisms and ion channel function. *J. Physiol.* **588**, 1823–1827 (2010).
3. Turrigiano, G. G. The self-tuning neuron: Synaptic scaling of excitatory synapses. *Cell* **135**, 422–435 (2008).
4. Iliff, J. J. *et al.* Cerebral arterial pulsation drives paravascular CSF-interstitial fluid exchange in the murine brain. *J. Neurosci.* **33**, 18190–18199 (2013).
5. Strazzullo, P. & Leclercq, C. Sodium. *Adv. Nutr.* **5**, 188–190 (2014).
6. Zacchia, M., Abategiovanni, M. L., Stratigis, S. & Capasso, G. Potassium: From physiology to clinical implications. *Kidney Dis.* **2**, 72–79 (2016).
7. Bezanilla, F., Rojas, E. & Taylor, R. E. Sodium and potassium conductance changes during a membrane action potential. *J. Physiol.* **211**, 729–751 (1970).
8. Amatniek, E., Freygang, W., Grundfest, H., Kiebel, G. & Shanes, A. The effect of temperature, potassium, and sodium on the conductance change accompanying the action potential in the squid giant axon. *J. Gen. Physiol.* **41**, 333–342 (1957).
9. Hodgkin, A. L. & Huxley, A. F. The components of membrane conductance in the giant axon of Loligo. *J. Physiol.* **116**, 473–496 (1952).
10. Ahern, C. A., Payandeh, J., Bosmans, F. & Chanda, B. The hitchhiker's guide to the voltage-gated sodium channel galaxy. *J. Gen. Physiol.* **147**, 1–24 (2016).
11. Bean, B. P. The action potential in mammalian central neurons. *Nat. Rev. Neurosci.* **8**, 451–465 (2007).
12. Luo, L. *et al.* Ion channels and transporters in microglial function in physiology and brain diseases. *Neurochem. Int.* **142**, 104925 (2021).
13. Min, R. & van der Knaap, M. S. Genetic defects disrupting glial ion and water homeostasis in the brain. *Brain Pathol.* **28**, 372–387 (2018).
14. Schwartzkroin, P. A., Baraban, S. C. & Hochman, D. W. Osmolarity, ionic flux, and changes in brain excitability. *Epilepsy Res.* **32**, 275–285 (1998).
15. Rust, P. & Ekmekcioglu, C. Impact of salt intake on the pathogenesis and treatment of hypertension. *Adv. Exp. Med. Biol.* **956**, 61–84 (2017).
16. Francis, C. K. Hypertension and cardiac disease in minorities. *Am. J. Med.* **88**, 3s–8s (1990).
17. Pistoia, F. *et al.* Hypertension and stroke: Epidemiological aspects and clinical evaluation. *High Blood Press. Cardiovasc. Prev.* **23**, 9–18 (2016).
18. Hussain, M. S. *et al.* Sodium imaging intensity increases with time after human ischemic stroke. *Ann. Neurol.* **66**, 55–62 (2009).

19. Baier, S. *et al.* Chlorine and sodium chemical shift imaging during acute stroke in a rat model at 9.4 Tesla. *Magn. Reson. Mater. Phys. Biol. Med.* **27**, 71–79 (2014).
20. Leftin, A. *et al.* Multiparametric classification of sub-acute ischemic stroke recovery with ultrafast diffusion, ^{23}Na, and MPIO-labeled stem cell MRI at 21.1 T. *NMR Biomed.* **33**, e4186 (2020).
21. Feigin, V. L., Lawes, C. M., Bennett, D. A. & Anderson, C. S. Stroke epidemiology: A review of population-based studies of incidence, prevalence, and case-fatality in the late 20th century. *Lancet Neurol.* **2**, 43–53 (2003).
22. Simmons, C. A., Poupore, N. & Nathaniel, T. I. Age stratification and stroke severity in the telestroke network. *J. Clin. Med.* **12**, 1519 (2023).
23. Oliveros, E. *et al.* Hypertension in older adults: Assessment, management, and challenges. *Clin. Cardiol.* **43**, 99–107 (2020).
24. Faraco, G. *et al.* Dietary salt promotes neurovascular and cognitive dysfunction through a gut-initiated TH17 response. *Nat. Neurosci.* **21**, 240–249 (2018).
25. Cheng, X. J., Gao, Y., Zhao, Y. W. & Cheng, X. D. Sodium chloride increases Aβ levels by suppressing aβ clearance in cultured cells. *PLoS One* **10**, e0130432 (2015).
26. Harrington, M. G. *et al.* Cerebrospinal fluid sodium increases in migraine. *Headache* **46**, 1128–1135 (2006).
27. Reetz, K. *et al.* Increased brain tissue sodium concentration in Huntington's Disease—a sodium imaging study at 4 T. *Neuroimage* **63**, 517–524 (2012).
28. Pogwizd, S. M., Sipido, K. R., Verdonck, F. & Bers, D. M. Intracellular Na in animal models of hypertrophy and heart failure: Contractile function and arrhythmogenesis. *Cardiovasc. Res.* **57**, 887–896 (2003).
29. Murphy, E. & Eisner, D. A. Regulation of intracellular and mitochondrial sodium in health and disease. *Circ. Res.* **104**, 292–303 (2009).
30. Leo, L. *et al.* Increased susceptibility to cortical spreading depression in the mouse model of familial hemiplegic migraine type 2. *PLoS Genet.* **7**, e1002129 (2011).
31. Shavlakadze, T. *et al.* Age-related gene expression signature in rats demonstrate early, late, and linear transcriptional changes from multiple tissues. *Cell Rep.* **28**, 3263–73.e3 (2019).
32. Andreollo, N. A., Santos, E. F., Araújo, M. R. & Lopes, L. R. Rat's age versus human's age: What is the relationship?. *Arq. Bras. Circ Dig.* **25**, 49–51 (2012).
33. Jackson, S. J. *et al.* Does age matter? The impact of rodent age on study outcomes. *Lab. Anim.* **51**, 160–169 (2017).
34. Uluc, K., Miranpuri, A., Kujoth, G. C., Akture, E. & Baskaya, M. K. Focal cerebral ischemia model by endovascular suture occlusion of the middle cerebral artery in the rat. *J. Vis. Exp.* https://doi.org/10.3791/1978-v (2011).
35. Strickland, M., Yacoubi-Loueslati, B., Bouhaouala-Zahar, B., Pender, S. L. F. & Larbi, A. Relationships between ion channels, mitochondrial functions and inflammation in human aging. *Front. Physiol.* **10**, 158 (2019).
36. Franceschi, C. *et al.* The continuum of aging and age-related diseases: Common mechanisms but different rates. *Front. Med.* **5**, 61 (2018).
37. Hartmann, A. *et al.* Ranking biomarkers of aging by citation profiling and effort scoring. *Front. Genet.* **12**, 686320 (2021).
38. He, F. J., Markandu, N. D., Sagnella, G. A., de Wardener, H. E. & MacGregor, G. A. Plasma sodium: Ignored and underestimated. *Hypertension* **45**, 98–102 (2005).
39. Stocker, S. D., Monahan, K. D. & Browning, K. N. Neurogenic and sympathoexcitatory actions of NaCl in hypertension. *Curr. Hypertens. Rep.* **15**, 538–546 (2013).
40. Kawano, Y. *et al.* Sodium and noradrenaline in cerebrospinal fluid and blood in salt-sensitive and non-salt-sensitive essential hypertension. *Clin. Exp. Pharmacol. Physiol.* **19**, 235–241 (1992).
41. Nakamura, K. & Cowley, A. Jr. Sequential changes of cerebrospinal fluid sodium during the development of hypertension in Dahl rats. *Hypertension* **13**, 243–249 (1989).
42. Yamashita, Y. *et al.* Cerebrospinal fluid sodium and enhanced hypertension in salt-loaded spontaneously hypertensive rats. *J. Hypertens.* **10**, 7 (1992).
43. Huang, B. S., Van Vliet, B. N. & Leenen, F. H. Increases in CSF [Na^+] precede the increases in blood pressure in Dahl S rats and SHR on a high-salt diet. *Am. J. Physiol. Heart Circ. Physiol.* **287**, H1160–H1166 (2004).
44. Ostchega, Y., Fryar, C. D., Nwankwo, T. & Nguyen, D. T. Hypertension prevalence among adults aged 18 and over: United States, 2017–2018. NCHS Data Brief (2020).
45. Feigin, V. L. *et al.* World Stroke Organization (WSO): Global stroke fact sheet 2022. *Int. J. Stroke* **17**, 18–29 (2022).
46. Medoff, H. S. & Bongiovanni, A. M. Age, sex and species variations on blood pressure in normal rats. *Am. J. Physiol. Legacy Content* **143**, 297–299 (1945).
47. Cosic, A. *et al.* Attenuated flow-induced dilatation of middle cerebral arteries is related to increased vascular oxidative stress in rats on a short-term high salt diet. *J. Physiol.* **594**, 4917–4931 (2016).
48. Schmidt-Pogoda, A. *et al.* Dietary salt promotes ischemic brain injury and is associated with parenchymal migrasome formation. *PLoS One* **13**, e0209871 (2018).
49. Bailey, E. L. *et al.* Effects of dietary salt on gene and protein expression in brain tissue of a model of sporadic small vessel disease. *Clin. Sci.* **132**, 1315–1328 (2018).
50. Shemin, D. & Dworkin, L. D. Sodium balance in renal failure. *Curr. Opin. Nephrol. Hypertens.* **6**, 128–132 (1997).
51. Martin, K., Tan, S.-J. & Toussaint, N. D. Total body sodium balance in chronic kidney disease. *Int. J. Nephrol.* **2021**, 7562357 (2021).
52. Koch, C. A. & Fulop, T. Clinical aspects of changes in water and sodium homeostasis in the elderly. *Rev. Endocr. Metab. Disord.* **18**, 49–66 (2017).
53. Begg, D. P. Disturbances of thirst and fluid balance associated with aging. *Physiol. Behav.* **178**, 28–34 (2017).
54. Molaschi, M. *et al.* Hypernatremic dehydration in the elderly on admission to hospital. *J. Nutr. Health Aging* **1**, 156–160 (1997).
55. Yu, F. H. & Catterall, W. A. Overview of the voltage-gated sodium channel family. *Genome Biol.* **4**, 207 (2003).
56. Felix, L., Delekate, A., Petzold, G. C. & Rose, C. R. Sodium fluctuations in astroglia and their potential impact on astrocyte function. *Front. Physiol.* **11**, 871 (2020).
57. Jones, S. C. *et al.* Stroke onset time using sodium MRI in rat focal cerebral ischemia. *Stroke* **37**, 883–888 (2006).
58. Bartha, R. *et al.* Sodium T2*-weighted MR imaging of acute focal cerebral ischemia in rabbits. *Magn. Reson. Imaging* **22**, 983–991 (2004).
59. Puig, B., Brenna, S. & Magnus, T. Molecular communication of a dying neuron in stroke. *Int. J. Mol. Sci.* **19**, 2834 (2018).
60. Shrivastava, A. N., Triller, A. & Melki, R. Cell biology and dynamics of Neuronal Na^+/K^+-ATPase in health and diseases. *Neuropharmacology* **169**, 107461 (2020).
61. Rose, C. R. & Verkhratsky, A. Sodium homeostasis and signalling: The core and the hub of astrocyte function. *Cell Calcium* **117**, 102817 (2023).
62. Staehr, C., Aalkjaer, C. & Matchkov, V. V. The vascular Na, K-ATPase: Clinical implications in stroke, migraine, and hypertension. *Clin. Sci.* **137**, 1595–1618 (2023).
63. Warren, K. E. *et al.* Movement of cerebrospinal fluid tracer into brain parenchyma and outflow to nasal mucosa is reduced at 24 h but not 2 weeks post-stroke in mice. *Fluids Barriers CNS* **20**, 27 (2023).
64. Kajiwara, S. *et al.* Persistent brain exposure to high sodium induces stroke onset by upregulation of cerebral microbleeds and oxidative stress in hypertensive rats. *Hypertens. Res.* **47**, 78–87 (2024).

65. Iwai, T. *et al.* Sodium accumulation during ischemia induces mitochondrial damage in perfused rat hearts. *Cardiovasc. Res.* **55**, 141–149 (2002).
66. Popa-Wagner, A. *et al.* Ageing as a risk factor for cerebral ischemia: Underlying mechanisms and therapy in animal models and in the clinic. *Mech. Ageing Dev.* **190**, 111312 (2020).
67. Meyer, M. M. *et al.* Cerebral sodium (^{23}Na) magnetic resonance imaging in patients with migraine—a case-control study. *Eur. Radiol.* **29**, 7055–7062 (2019).
68. Abad, N., Rosenberg, J. T., Hike, D. C., Harrington, M. G. & Grant, S. C. Dynamic sodium imaging at ultra-high field reveals progression in a preclinical migraine model. *Pain* **159**, 2058–2065 (2018).
69. Vitvitsky, V. M., Garg, S. K., Keep, R. F., Albin, R. L. & Banerjee, R. Na^+ and K^+ ion imbalances in Alzheimer's disease. *Biochim. Biophys. Acta* **1822**, 1671–1681 (2012).
70. Mohan, D. *et al.* Link between dietary sodium intake, cognitive function, and dementia risk in middle-aged and older adults: A systematic review. *J. Alzheimers Dis.* **76**, 1347–1373 (2020).
71. Haeger, A. *et al.* What can 7T sodium MRI tell us about cellular energy depletion and neurotransmission in Alzheimer's disease?. *Alzheimers Dement.* **17**, 1843–1854 (2021).

Acknowledgements

The authors would like to thank all the staff from the Analytical Biochemistry Core and animal facility at HMRI.

Author contributions

The conception and study design involved A.F., A.V., X.A., and R.A.K. W.D., C.X., J.C., and X.A. performed tissue collection. X.W. and D.S. prepared the sample for the IC test. C.X., N.A., N.D., and A.F. were involved in method design for the ion tests. C.X. analyzed the data and designed the figures. C.X. and X.A. drafted the manuscript, and C.X., V.A., N.A., N.D., A.F., X.A., and R.A.K. performed critical revisions of it. All authors read and approved the final manuscript.

Funding

This study was supported by the W.M. Keck Foundation and NIH/NINDS R01NS072497.

Competing interests

The authors declare no competing interests.

Additional information

Correspondence and requests for materials should be addressed to X.A.